Author Manuscript

Author Manuscript

Author Manuscript

Author Manuscript

HHS Public Access

Author manuscript

Immunity. Author manuscript; available in PMC 2017 July 19.

Published in final edited form as:

Immunity. 2016 July 19; 45(1): 185–197. doi:10.1016/j.immuni.2016.06.027.

Ikaros Inhibits Group 3 Innate Lymphoid Cell Development and Function by Suppressing the Aryl Hydrocarbon Receptor Pathway

Shiyang Li[1,2,7,*], **Jennifer J. Heller**[1,2,*], **John W. Bostick**[1,2,3], **Aileen Lee**[1,2], **Hilde Schjerven**[4], **Philippe Kastner**[5], **Susan Chan**[5], **Zongming E. Chen**[6], and **Liang Zhou**[1,2,7]

[1]Department of Pathology, Feinberg School of Medicine, Northwestern University, Chicago, IL 60611, USA

[2]Department of Microbiology-Immunology, Feinberg School of Medicine, Northwestern University, Chicago, IL 60611, USA

[3]Department of Chemical and Biological Engineering, McCormick School of Engineering, Northwestern University, Evanston, IL 60208, USA

[4]Department of Laboratory Medicine, UCSF School of Medicine, San Francisco, CA, United States

[5]Institut de Génétique et de Biologie Moléculaire et Cellulaire (IGBMC), INSERM U964, CNRS UMR 7104, Université de Strasbourg, 67404 Illkirch, France

[6]Department of Laboratory Medicine in Geisinger Health System, 100 N. Academy Ave., MC 19-20, Danville, PA 17822

[7]Department of Infectious Diseases and Pathology, College of Veterinary Medicine, The University of Florida, Gainesville, FL 32608, USA

Abstract

Group 3 innate lymphoid cells (ILC3s) expressing the transcription factor (TF) RORγt are important for the defense and homeostasis of host intestinal tissues. The zinc finger TF Ikaros encoded by *Ikzf1* is essential for RORγt$^+$ fetal lymphoid tissue inducer (LTi) cell development and lymphoid organogenesis, but its role in postnatal ILC3s is unknown. Here, we showed that small intestinal ILC3s had the lowest expression of Ikaros compared to ILC precursors and other ILC subsets. Ikaros inhibited ILC3s in a cell-intrinsic manner through zinc finger-dependent inhibition

Correspondence: Liang Zhou, Tel: 352-294-8293; Fax: 352-392-9704; liangzhou497@ufl.edu.
*These authors contribute equally

Author Contributions

S.L., J.J.H, A.L., H.S. designed the study and did experiments. J.W.B. contributed to the data analysis. H.S., P.K. and S.C. provided reagents and suggestions. Z.E.C performed histological analysis. S.L. and L.Z. wrote the papers with the input from all authors. L.Z. conceived and coordinated the project.

The author has no financial conflict of interest.

Publisher's Disclaimer: This is a PDF file of an unedited manuscript that has been accepted for publication. As a service to our customers we are providing this early version of the manuscript. The manuscript will undergo copyediting, typesetting, and review of the resulting proof before it is published in its final citable form. Please note that during the production process errors may be discovered which could affect the content, and all legal disclaimers that apply to the journal pertain.

Author Manuscript Author Manuscript Author Manuscript Author Manuscript

of transcriptional activity of the aryl hydrocarbon receptor, a key regulator of ILC3 maintenance and function. Ablation of *Ikzf1* in RORγt$^+$ ILC3s resulted in increased expansion and cytokine production of intestinal ILC3s and protection against infection and colitis. Therefore, in contrast to its requirement for LTi development, Ikaros inhibits postnatal ILC3 development and function to regulate gut immune responses at steady state and in disease.

eTOC Blurb

Ikaros is necessary for fetal lymphoid tissue inducer cell development, but its role in postnatal ILC3s is unknown. Zhou and colleagues demonstrate that Ikaros negatively regulates ILC3 development and function by suppressing Ahr transcriptional activity. These findings indicate that Ikaros-mediated regulation of gut immunity occurs in a cell type-specific manner.

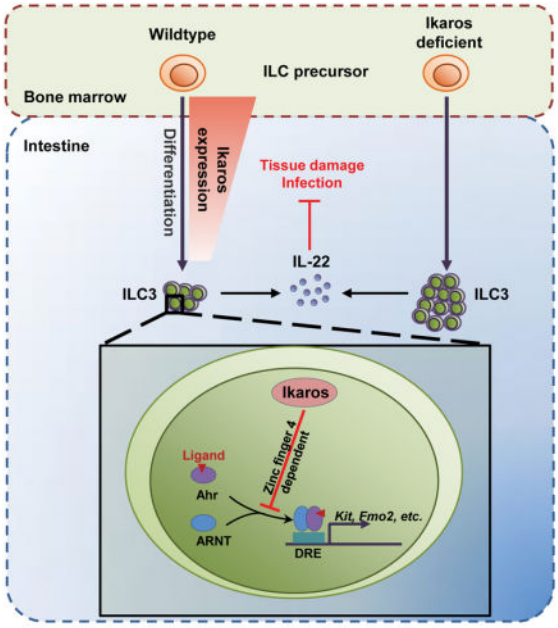

Introduction

Group 3 innate lymphoid cells (ILC3s) expressing the transcription factor (TF) RORγt are involved in maintaining intestinal homeostasis by protecting the host from pathogen infections, controlling the gut microflora, and contributing to the development of gut lymphoid tissues like cryptopatches (Artis and Spits, 2015). Disruption of the ILC3 compartment is associated with the occurrence of inflammatory bowel disease (IBD) and can result in susceptibility to gut infection, such as *Citrobacter rodentium*, a mouse pathogen that models human pathogenic *Escherichia coli* infection (McKenzie et al., 2014; Pearson et al., 2012). Control of *C. rodentium* infection requires both innate and adaptive immunity, such as ILC3s, T helper 17 (Th17) cells, and Th22 cells (Basu et al., 2012; Song et al., 2015; Sonnenberg et al., 2011). Production of effector cytokine interleukin 22 (IL-22) by ILC3s and T cells is important for host defense during pathogenic bacterial infection and for shaping host commensal microbiota (Rutz et al., 2014). Innate and adaptive immune cells

Author Manuscript Author Manuscript Author Manuscript Author Manuscript

including ILC3s and T cells can also provide protection against gut inflammation caused by tissue damage (e.g., Dextran Sulfate Sodium (DSS)-induced colitis), at least in part through the action of the effector cytokines IL-22 and IL-17 to maintain gut epithelial integrity (Lee et al., 2015; Sawa et al., 2011; Sugimoto et al., 2008).

The aryl hydrocarbon receptor (Ahr) is a ligand-dependent environmental sensor and its transcriptional activity requires ligand-induced nuclear translocation and dimerization with its partner, the aryl hydrocarbon receptor nuclear translocator (ARNT) (Fukunaga et al., 1995). Ahr is essential for the postnatal accumulation of ILC3s and for the gut immunity during microbial infections (Kiss et al., 2011; Lee et al., 2012; Qiu et al., 2012; Zelante et al., 2013). There are multiple mechanisms of action of Ahr in ILC3 maintenance, for example, through promotion of cell survival, proliferation, and/or Notch-dependent pathways in ILC3s (Kiss et al., 2011; Lee et al., 2012; Qiu et al., 2012). In addition, recruitment of Ahr to ILC3 target gene *Il22* requires RORγt, presumably mediated by protein-protein interaction between Ahr and RORγt (Qiu et al., 2012). However, how Ahr activity is regulated during ILC3 development is unknown.

ILC3s, together with the other two subsets of innate lymphoid cells, ILC1s and ILC2s, are derived from a common lymphoid progenitor (CLP) in the bone marrow (Artis and Spits, 2015). CLP gives rise to the common helper innate lymphoid progenitor (CHILP), which has the potential to differentiate into all the ILC subsets, except conventional NK cells (Serafini et al., 2015). In contrast to postnatal ILC3s, fetal lymphoid tissue-inducing (LTi) cells in which RORγt is also highly expressed are derived from the fetal liver (Kim et al., 2009). Distinct modes of transcriptional regulation of postnatal ILC3s and fetal LTi cells occur; for instance, Notch signaling is required for adult ILC3s but not fetal LTi cell development (Possot et al., 2011). Similarly, Ahr is not needed for fetal LTi cells or lymphoid organogenesis such as lymph node formation, while Ahr deficiency results in a significant decrease of ILC3s and cryptopatches after birth (Kiss et al., 2011; Lee et al., 2012; Qiu et al., 2012).

The C2H2 zinc finger transcription factor Ikaros is a key regulator of hematopoiesis, including the development of fetal T cells, B cells, and natural killer cells by affecting CLP, pro-B cells, and NK precursors (Yoshida et al., 2010). Additionally, Ikaros is crucial for the generation of secondary lymphoid organs (e.g., lymph nodes and Peyer's Patches), through its role in promoting fetal LTi cells (Schjerven et al., 2013; Wang et al., 1996). However, it remains unclear whether Ikaros plays a similar role in the development and function of postnatal ILC3s, including LTi-like cells without the expression of natural cytotoxicity receptor NKp46 (NKp46^{-}ILC3s) and ILC3s with the expression of NKp46 (NKp46^{+}ILC3s). Here, we showed that Ikaros played a differential role in fetal and postnatal ILC3 development. Ikaros negatively regulated postnatal ILC3s in the gut by inhibiting Ahr activity. Our data suggest that downregulation of Ikaros represents a cell-intrinsic requirement for normal ILC3 lineage specification and expansion, and is beneficial to host immunity during infection and inflammation.

Author Manuscript Author Manuscript Author Manuscript Author Manuscript

Result

Reduced expression of Ikaros in ILC3 compartment

Although Ikaros is required for fetal LTi cells and postnatal CLP generation, the role of Ikaros in the development of gut ILCs, which are thought to originate from CLP and subsequently from CHILP (Artis and Spits, 2015), is unknown. As Ikaros is ubiquitously expressed in hematopoietic cells (Georgopoulos et al., 1994), we analyzed the expression of Ikaros by ILC precursors in the bone marrow (CLP, CHILP, and ILC2 progenitor (ILC2P)) and by mature ILC subsets in the gut (ILC1s, ILC2s, and ILC3s) (Figure S1A). Compared to other cell populations, ILC3s expressed the lowest amounts of Ikaros protein and mRNA, as measured by intracellular staining and realtime RT-PCR (Figures 1A, 1B, and S1B). In addition, lower amounts of Ikaros protein were found in ILC3s in the small intestine than the large intestine, which might be related with the expansion of ILC3s in the small intestine (Figures 1C to 1E). These data prompted us to hypothesize that downregulation of Ikaros might represent an important molecular event for ILC3 lineage specification and expansion.

Ikaros inhibits postnatal ILC3 accumulation in the gut

To investigate the role of Ikaros in gut ILC3s, we utilized mice with germline-targeted deletion of the *Ikzf1* exon encoding zinc finger 4 ($Ikzf1^{\Delta F4/\Delta F4}$) on a C57BL/6 genetic background (Schjerven et al., 2013). Unlike mice with germline-targeted deletion of the *Ikzf1* exon encoding zinc finger 1 ($Ikzf1^{\Delta F4/\Delta F4}$) that have normal fetal LTi compartment and lymphoid organogenesis, $Ikzf1^{\Delta F4/\Delta F4}$ mice phenocopy the Ikaros null mice ($Ikzf1^{-/-}$) in respect to deficiency in fetal LTi cells and secondary lymphoid tissues (e.g., lymph nodes and Peyer's Patches) (Schjerven et al., 2013; Wang et al., 1996). Further analyses reveal that $Ikzf1^{\Delta F4/\Delta F4}$ mice have a substantial loss of DNA-binding activity, which is consistent with lack-of-function of Ikaros in specific immune aspects of this mouse strain (Schjerven et al., 2013). In sharp contrast to the lack of fetal LTi cells, we observed a marked increase in frequency and number of RORγt$^+$ ILC3s, including NKp46$^+$ ILC3s (CD3$^-$NKp46$^+$RORγt$^+$ cells), and LTi-like cells with CD4 (CD3$^-$NKp46$^-$CD4$^+$RORγt$^+$ cells) or without CD4 expression (CD3$^-$NKp46$^-$CD4$^-$RORγt$^+$ cells) in the intestine of adult $Ikzf1^{\Delta F4/\Delta F4}$mice (Figures 1F to 1I). In the intestine under the steady state, ILC3s are the major producers of IL-22, a key cytokine to protect the host from pathogenic inflammation and colitis (Artis and Spits, 2015). Accordingly, we found more IL-22-producing ILC3s in $Ikzf1^{\Delta F4/\Delta F4}$ mice, suggesting that these ILC3s were functional (Figures S1C and S1D). Of note, the increased ILC3 compartment was only apparent in $Ikzf1^{\Delta F4/\Delta F4}$ mice, but not in $Ikzf1^{\Delta F4/\Delta F4}$ mice (data not shown), suggesting an important role for Ikaros zinc finger 4 in the regulation of ILC3s. We also observed higher proliferation of ILC3s revealed by Ki67 staining in $Ikzf1^{\Delta F4/\Delta F4}$ mice, consistent with increased ILC3s in the gut (Figure 1J). Together, these data suggest that Ikaros functions as a suppressor of the accumulation of ILC3s in the gut, and its downregulation during development may relieve Ikaros' inhibition of ILC3 lineage.

Ikaros regulates ILC3 ontogeny

Postnatally-developed cryptopatches located at the base of the villi in the intestine are mainly populated by RORγt-expressing ILC3s (Kanamori et al., 1996; Serafini et al., 2015). Consistent with the increase of ILC3s in the gut, there was a 3-fold increase in the number

Author Manuscript Author Manuscript Author Manuscript Author Manuscript

of cryptopatches both in the small and large intestines of *Ikzf1*$^{\Delta F4/\Delta F4}$ mice compared to wildtype littermate mice (Figures 2A and 2B). The chemokine receptor CCR6, mainly expressed by NKp46^{-} ILC3s (i.e., LTi-like cells), is required for the formation of cryptopatches (Bouskra et al., 2008; Lugering et al., 2010). In accordance with the higher number of observed cryptopatches, both the percentage and number of CCR6^{+} ILC3s in *Ikzf1*$^{\Delta F4/\Delta F4}$ mice were markedly elevated (Figures 2C and 2D).

We next investigated the ontogeny of ILC3s in *Ikzf1*$^{\Delta F4/\Delta F4}$ mice after birth. Substantial defects in intestinal ILC3s were evident in newborn *Ikzf1*$^{\Delta F4/\Delta F4}$ mice (day 0), consistent with the lack of fetal LTi cells caused by Ikaros deficiency (Figures 2E and 2F) (Schjerven et al., 2013). However, one week-old *Ikzf1*$^{\Delta F4/\Delta F4}$ mice started to show increased frequency of RORγt^{+} ILC3s, especially NKp46^{-} ILC3s, in both the small and large intestines, while the increase of NKp46^{+} ILC3s became more evident at 3 weeks after birth (Figures 2E and 2F). Given the expansion of commensal flora after birth, we next assessed the contribution of microbiota to the increase of ILC3s in *Ikzf1*$^{\Delta F4/\Delta F4}$ mice. Although antibiotic treatment reduced the gut Th17 cells as reported (Figures S2A and S2B) (Ivanov et al., 2008), depletion of gut microbiota by antibiotics did not reduce the frequency of ILC3s in *Ikzf1*$^{\Delta F4/\Delta F4}$ mice (Figures S2C and S2D), demonstrating a microbiota-independent upregulation of ILC3s in the absence of wildtype full-length Ikaros. Together, these data indicate that in contrast to its requirement for fetal ILC3s, Ikaros inhibits postnatal ILC3 development.

Ikaros negatively regulates postnatal ILC3s in a cell-intrinsic manner

Ikaros is expressed by multiple hematopoietic cell populations (Georgopoulos et al., 1994). We next investigated whether Ikaros regulated ILC3s cell intrinsically. We crossed mice with loxP-flanked alleles of *Ikzf1* exon 8 that encodes C-terminal zinc finger dimerization domain (Heizmann et al., 2013) with transgenic mice expressing of *Rorc*-driven Cre recombinase to specifically delete Ikaros in RORγt-expressing cells (i.e., ILC3s and T cells). The deletion efficiency of Ikaros was confirmed by intracellular staining of Ikaros in ILC3s and T cells (Figure 3A). Similar to *Ikzf1*$^{\Delta F4/\Delta F4}$ mice, *Ikzf1*$^{f/f}$ *Rorc*-cre mice showed increased percentages of ILC3s (Figures 3B and 3C). The *Cd4-cre* transgene only functions in T cells but not in RORγt^{+} ILC3s despite the expression of CD4 in some adult LTi-like cells, presumably due to the lack of *cis*-acting elements that are crucial for LTi or LTi-like cells in the *Cd4* transgene driving Cre expression (Ivanov et al., 2006). In agreement with this, the ILC3 compartment in the gut was not affected in *Ikzf1*$^{f/f}$ *Cd4*-cre mice (Figures 3D and 3E), in which Ikaros was only ablated in T cells (Figure 3A). Similar to *Ikzf1*$^{\Delta F4/\Delta F4}$ mice (Figure 2), the number of cryptopatches in both the small and large intestines of *Ikzf1*$^{f/f}$ *Rorc*-cre mice was increased compared to wildtype littermate mice (Figures S2E and S2F). However, in contrast to *Ikzf1*$^{\Delta F4/\Delta F4}$ mice, *Ikzf1*$^{f/f}$ *Rorc*-cre mice exhibited normal lymphoid tissue development, such as Peyer's patches and lymph nodes (Figure S2G). Together, these data suggest that the regulation of postnatal ILC3s by Ikaros is cell-intrinsic.

Ahr is required for the upregulation of ILC3s in the gut of *Ikzf1*$^{\Delta F4/\Delta F4}$ mice

Ahr has been shown to function as a key transcription factor for the maintenance of adult ILC3s (Kiss et al., 2011; Lee et al., 2012; Qiu et al., 2012). We hypothesized that Ikaros may

Author Manuscript Author Manuscript Author Manuscript Author Manuscript

regulate Ahr expression and/or function in ILC3s. Although the expression of Ahr-regulated genes (Dere et al., 2011) was increased in *Ikzf1*$^{\Delta F4/\Delta F4}$ ILC3s, the *Ahr* mRNA remained unchanged in *Ikzf1*$^{\Delta F4/\Delta F4}$ ILC3s (Figure S3A). Thus, we sought to investigate the requirement of Ahr pathway in upregulation of ILC3 compartment in *Ikzf1*$^{\Delta F4/\Delta F4}$ mice. We generated *Ikzf1*$^{\Delta F4/\Delta F4}$*Ahr*$^{-/-}$ mice to genetically ablate Ahr in *Ikzf1*$^{\Delta F4/\Delta F4}$ mice. The increase in the frequency of ILC3s was completely abolished in *Ikzf1*$^{\Delta F4/\Delta F4}$*Ahr*$^{-/-}$ mice as well as in *Ikzf1*$^{\Delta F4/+}$*Ahr*$^{-/-}$ controls (Figures 4A and 4B), suggesting that similar to its essential role in regulating adult ILC3s (Kiss et al., 2011; Lee et al., 2012; Qiu et al., 2012), Ahr is indispensable for the increase in the frequency of ILC3s in *Ikzf1*$^{\Delta F4/\Delta F4}$ mice.

Ahr has been reported to be critical for proliferation and IL-22 production of ILC3s (Kiss et al., 2011; Lee et al., 2012; Qiu et al., 2012). Therefore, we wanted to determine the post-developmental role of Ahr in *Ikzf1*$^{\Delta F4/\Delta F4}$ ILC3s. Large intestinal LPLs were isolated and cultured in the presence of the Ahr ligand 6-formylindolo[3,2-b]carbazole (FICZ) or the Ahr antagonist that was previously used (Gagliani et al., 2015). The proliferation of wildtype and *Ikzf1*$^{\Delta F4/\Delta F4}$ ILC3s revealed by Ki-67 staining was increased by FICZ but inhibited by Ahr antagonist (Figures S3B and S3C), consistent with the role of Ahr activation in promoting ILC3 proliferation (Kiss et al., 2011). Although IL-22^{+} ILC3s were increased in *Ikzf1*$^{\Delta F4/\Delta F4}$ mice (Figures S1C and S1D), there was no significant increase in IL-22 production in *Ikzf1*$^{\Delta F4/\Delta F4}$ ILC3s on a per cell basis, and FICZ had little effect on IL-22 production in wildtype or *Ikzf1*$^{\Delta F4/\Delta F4}$ ILC3s (Figures S3D and S3E). In contrast, treatment of the Ahr antagonist could markedly inhibit IL-22 (Figures S3D and S3E), consistent with the requirement of Ahr for ILC3 function (e.g., production of IL-22) (Kiss et al., 2011; Lee et al., 2012; Qiu et al., 2012). Together, genetic and pharmacological data suggest that the activation of Ahr pathway was a key molecular event responsible for the expansion of Ikaros-deficient ILC3s.

Ikaros interacts with Ahr and regulates the dimerization between Ahr and ARNT

We next investigated the potential crosstalk between Ikaros and Ahr in the regulation of ILC3 compartment. Using proximity ligation assay (PLA), a fluorescence-based technique that allows the detection of protein-protein interaction based on physical proximity (Weibrecht et al., 2010), interaction between Ikaros and Ahr was detected as immunofluorescence dots in wildtype CD3^{-}CD45^{low}CD90^{hi} cells that mainly consist of ILC3s in the gut (Guo et al., 2014), while minimal positive signals were observed in cells from *Ikzf1*$^{\Delta F4/\Delta F4}$ mice (Figure 4C). The antibody against Ikaros used for PLA recognized both full-length Ikaros and Ikaros lacking zinc finger 4 in ILC3s (Figure S3F), suggesting that the substantial decrease of PLA signals was not due to biased binding of primary antibody. Consistent with PLA results, the interaction between Ahr and full-length Ikaros was also demonstrated by co-immunoprecipitation in HEK293T cells (Figures 4D and S4A). Ikaros that lacks zinc finger 4 had no effect on its interaction with ATP-dependent nucleosome remodeling protein Mi2β (data not shown) (Koipally and Georgopoulos, 2002; Sridharan and Smale, 2007), but lost its association with Ahr, while Ikaros lacking zinc finger 1 retained its ability to interact with Ahr (Figure S4A).

Author Manuscript Author Manuscript Author Manuscript Author Manuscript

Domain-mapping of Ahr showed that its PAS-A domain was responsible for Ahr-Ikaros interaction (Figures S4B and S4C). It has been demonstrated that the transcriptional function of Ahr requires dimerization with its partner, the aryl hydrocarbon receptor nuclear translocator (ARNT), through the PAS-A domain (Wu et al., 2013). We then wondered whether Ikaros would play a role in Ahr-ARNT dimerization. Upon stimulation with the Ahr ligand FICZ, Ahr showed enhanced binding with ARNT (Figure 4D). Forced expression of full-length Ikaros in a dose-dependent manner markedly suppressed the dimerization of Ahr and ARNT (Figures 4D and S4D), while expression of Ikaros lacking zinc finger 4 failed to do so (Figure 4D). As cell scarcity prevented us from examining the role of Ikaros in primary ILC3s biochemically, we took advantage of T cells that share similarity to ILCs in transcriptional regulation. We investigated the binding of endogenous Ahr and ARNT in primary Th17 cells differentiated in vitro from wildtype or *Ikzf1*$^{\Delta F4/\Delta F4}$ mice. Ahr protein level was decreased in *Ikzf1*$^{\Delta F4/\Delta F4}$ Th17 cells (Figure S4E), consistent with our previous study (Heller et al., 2014). However, enhanced binding between Ahr and ARNT was observed in these cells after normalization of Ahr protein expression, supporting that Ikaros may perturb Ahr-ARNT dimerization (Figure S4E). It has been shown that the Ahr-ARNT heterodimer can bind to and promote the transcription of Dioxin Responsive Element (DRE)-containing genes (Stockinger et al., 2014). Indeed, full-length Ikaros suppressed the FICZ-induced DRE-driven luciferase activity, whereas Ikaros lacking zinc finger 4 lost the suppressive ability (Figure S4F). We also observed increased expression of *Kit* in *Ikzf1*$^{\Delta F4/\Delta F4}$ ILC3s, consistent with the observation that *Kit* was a DRE-containing gene regulated by Ahr in ILC3s (Figure S3A) (Kiss et al., 2011). Additionally, Ahr-ChIP revealed increased enrichment of Ahr binding at its target genes, such as *Kit* and *Fmo2* (Dere et al., 2011; Kiss et al., 2011), in gut ILC3s of *Ikzf1*$^{\Delta F4/\Delta F4}$ mice (Figure 4E), consistent with the enhanced transcriptional activity of Ahr. Together, these data demonstrate that Ikaros negatively regulates Ahr transcriptional activity through blocking Ahr-ARNT interaction in a zinc finger 4-dependent manner.

Ikaros regulates gut immunity to *Citrobacter rodentium* infection in a cell type-specific manner

Control of *C. rodentium* infection in mice, which resembles attaching and effacing *E. coli* infection in humans, requires coordinated actions of the innate and adaptive immune systems (Collins et al., 2014). Consistent with the protective role of Th22 cells in *C. rodentium* infection (Basu et al., 2012), our previous data suggest that adoptive transfer of *Ikzf1*$^{\Delta F4/\Delta F4}$ T cells can more efficiently protect the host from the infection due to elevated IL-22 production (Heller et al., 2014). Given the upregulation of IL-22^{+} ILC3s in *Ikzf1*$^{\Delta F4/\Delta F4}$ mice, we next investigated the role of Ikaros in gut immunity during *C. rodentium* infection.

To this end, we adoptively transferred gut ILC3s purified from either *Ikzf1*$^{\Delta F4/\Delta F4}$ or wildtype mice into RORγt-deficient mice (*Rorc*$^{gfp/gfp}$), in which no ILC3s exist and most if not all Th22 and Th17 cells are absent, to determine whether *Ikzf1*$^{\Delta F4/\Delta F4}$ ILC3s could provide early protection in *Rorc*$^{gfp/gfp}$ mice. At day 4 post infection, *Rorc*$^{gfp/gfp}$ mice without adoptive transfer exhibited approximately 10-fold higher bacterial colony-forming units (CFUs) of *C. rodentium* in their feces than wildtype C57BL/6 mice (Figure 5A). In

Author Manuscript Author Manuscript Author Manuscript Author Manuscript

contrast, *Rorc*$^{gfp/gfp}$ mice receiving ILC3s had a significant decrease of bacterial load in their feces (Figure 5A). *Rorc*$^{gfp/gfp}$ mice receiving *Ikzf1*$^{\Delta F4/\Delta F4}$ ILC3s controlled bacterial load even better than those receiving wildtype ILC3s (Figure 5A). The protection from ILC3s ameliorated the weight loss significantly and prevented these mice from early death (Figures 5B and 5C). However, at day 9, *Rorc*$^{gfp/gfp}$ mice receiving either wildtype or *Ikzf1*$^{\Delta F4/\Delta F4}$ ILC3s had higher CFUs of *C. rodentium*, highlighting the indispensable role of adaptive Th22 and Th17 cells in eliminating the infection (Figure S5A). Although the same number of donor ILC3s was adoptively transferred, *Ikzf1*$^{\Delta F4/\Delta F4}$ ILC3s showed higher accumulation in the lamina propria of *Rorc*$^{gfp/gfp}$ mice than wildtype ILC3s (Figure S5B), and more IL-22-producing *Ikzf1*$^{\Delta F4/\Delta F4}$ ILC3s were also observed (Figure S5C). These data were corroborated by the observation that *Ikzf1*$^{\Delta F4/\Delta F4}$ ILC3s exhibited increased proliferation revealed by Ki67 staining compared to wildtype ILC3s in the gut (Figure S5D).

To further determine the cell-intrinsic mechanisms of Ikaros, we subjected three mouse genetic models that alter or ablate Ikaros expression in different cell compartments (i.e., *Ikzf1*$^{\Delta F4/\Delta F4}$ mice, *Ikzf1*$^{f/f}$ *Rorc*-cre mice, and *Ikzf1*$^{f/f}$ *Cd4*-cre mice) to *C. rodentium* infection. At day 4 post *C. rodentium* infection when innate responses are more prevalent compared to day 9 post infection (Figures 5D to 5F), IL-22^{+} ILC3s were markedly enhanced in *Ikzf1*$^{\Delta F4/\Delta F4}$ mice and *Ikzf1*$^{f/f}$ *Rorc*-cre mice, but not in *Ikzf1*$^{f/f}$ *Cd4*-cre mice (Figures 5D to 5F). Compared to their wildtype littermate mice, *Ikzf1*$^{\Delta F4/\Delta F4}$ and *Ikzf1*$^{f/f}$ *Rorc*-cre mice controlled bacterial infection more efficiently with reduced bacterial load (CFU counts) in feces at Day 4 (Figures 5G to 5I), consistent with enhanced ILC3-mediated immune responses. Together, these data support the conclusion that Ikaros regulates ILC3s cell-intrinsically during infection.

A complex role of Ikaros in regulation of T cell responses emerged when we examined the mice under the steady state and during *C. rodentium* infection. Without infection, all three Ikaros-targeted mice showed enhanced production of IL-22 by T cells under the steady state (Figure S6, and data not shown (Heller et al., 2014)), consistent with the role of Ikaros in suppressing Th22 cells (Heller et al., 2014). However, during *C. rodentium* infection, at day 9 when T cell responses were pronounced in wildtype littermate mice (Figures 5D to 5F and S7A to S7C), IL-22 and IL-17 expression by T cells were significantly reduced in *Ikzf1*$^{\Delta F4/\Delta F4}$ mice and *Ikzf1*$^{f/f}$ *Cd4*-cre mice and to a less extent in *Ikzf1*$^{f/f}$ *Rorc*-cre mice (Figures 5D to 5E and S7A to S7C). Despite the reduced T cell responses at day 9 after *C. rodentium* infection, *Ikzf1*$^{\Delta F4/\Delta F4}$ mice but not *Ikzf1*$^{f/f}$ *Cd4*-cre or *Ikzf1*$^{f/f}$ *Rorc*-cre mice showed progressive weight loss with high CFU counts in feces at day 9 after infection (Figures S7D to S7F and 5G to 5I). Increased IL-22^{+} ILC3s and/or elevated steady-state IL-22/IL-17 expression by T cells in *Ikzf1*$^{f/f}$ *Rorc*-cre mice or *Ikzf1*$^{f/f}$ *Cd4*-cre mice may contribute to anti-bacterial immunity and control of *C. rodentium.* However, other yet-to-be defined mechanisms may be responsible for reduced T cell responses at the late stage of infection in *Ikzf1*$^{f/f}$ *Rorc*-cre mice or *Ikzf1*$^{f/f}$ *Cd4*-cre mice, which nevertheless maintain efficient control of *C. rodentium*.

These data are in sharp contrast to our previous data showing enhanced anti-bacterial immunity mediated by Th22 cells in *Rag*1$^{-/-}$ mice after adoptive transfer of *Ikzf1*$^{\Delta F4/\Delta F4}$ CD4^{+} T cells, in which the innate immune system is presumably intact in the *Rag1*$^{-/-}$

Author Manuscript Author Manuscript Author Manuscript Author Manuscript

recipients (Heller et al., 2014). These paradoxical effects of Ikaros in regulation of T cell responses may be due to the contribution of Ikaros in other cellular compartments that are potentially altered under the steady state or during infection. Consistent with the crucial role of dendritic cells (DCs) in controlling *C. rodentium* (Schreiber et al., 2013), *Ikzf1*$^{\Delta F4/\Delta F4}$ mice showed a marked reduction of DCs (Figure S7G), supporting the regulation of DCs by Ikaros (Wu et al., 1997). Although we cannot rule out the possibility that specific aspects of DCs (certain subsets and/or function) might be affected in *Ikzf1*$^{f/f}$ *Rorc*-cre mice or *Ikzf1*$^{f/f}$ *Cd4*-cre mice during infection, no apparently numerical perturbation of DC compartment was observed in either *Ikzf1*$^{f/f}$ *Rorc*-cre mice or *Ikzf1*$^{f/f}$ *Cd4*-cre mice (Figures S7H and S7I), consistent with *Rorc*-cre and *Cd4*-cre-restricted deletion in lymphocyte lineages.

Deletion of Ikaros in ILC3s protects mice from DSS-induced colitis

To further corroborate our findings of regulation of ILC3s by Ikaros, we used DSS-induced innate colitis model to determine the role of Ikaros in ILC3s during gut inflammation. While *Ikzf1*$^{f/f}$ *Cd4*-cre mice had similar weight loss kinetics, colon length and pathohistological changes in the colon to those of wildtype littermate controls, both *Ikzf1*$^{\Delta F4/\Delta F4}$ mice and *Ikzf1*$^{f/f}$ *Rorc*-cre mice showed higher resistance to DSS treatment (Figure 6), suggesting that deletion of Ikaros in ILC3s protects the mice from DSS-induced colitis. Accordingly, enhanced IL-22^{+} ILC3s and IL-17^{+} ILC3s were observed in *Ikzf1*$^{\Delta F4/\Delta F4}$ mice and *Ikzf1*$^{f/f}$ *Rorc*-cre mice (Figures 7A and 7B), consistent with the protective role of IL-22 and IL-17 in DSS-induced colitis (Lee et al., 2015; Sawa et al., 2011; Sugimoto et al., 2008). Granulocyte-macrophage colony-stimulating factor (GM-CSF)-producing ILC3s also increased in *Ikzf1*$^{\Delta F4/\Delta F4}$ mice and *Ikzf1*$^{f/f}$ *Rorc*-cre mice in DSS-induced colitis despite the inflammatory role of GM-CSF in certain innate colitis model (i.e., anti-CD40 model) (Figure 7C) (Song et al., 2015). These data collectively indicate that Ikaros negatively regulates ILC3 function during colitis, and inhibition of Ikaros in ILC3s may alleviate gut tissue damage.

Discussion

Our results showed that downregulation of Ikaros expression during development favored ILC3 lineage specification and expansion. This conclusion was consistent with the observation that ILC3s expressed lower amounts of Ikaros compared to their progenitors or other ILC subsets. The wildtype level and/or function of Ikaros may be important to keep the ILC3-mediated immune responses in check to maintain gut homeostasis under the steady state. However, during infection and inflammation, inhibition of Ikaros expression or function resulted in enhanced ILC3s in the gut, thus beneficial in certain disease settings to the host immunity.

Ikaros played a differential role in fetal versus postnatal ILC3 development. Our data showed that it acted as a suppressor of the development of postnatal ILC3s via its zinc finger 4, in contrast to its function in promoting fetal LTi cells (Schjerven et al., 2013; Wang et al., 1996). Despite the expression of RORγt in fetal LTi cells, *Ikzf1*$^{f/f}$ *Rorc*-cre mice had normal development of lymph nodes and Peyer's patches, in contrast to *Ikzf1*$^{-/-}$ mice or *Ikzf1*$^{\Delta F4/\Delta F4}$ mice. These data suggested sufficient amounts of Ikaros remaining for

Author Manuscript Author Manuscript Author Manuscript Author Manuscript

secondary lymphoid organogenesis after *Rorc*-cre mediated *Ikzf1* gene ablation, or a dispensable role for Ikaros in regulation of fetal LTi cells after induction of *Rorc* transcription during development.

Our data showed that Ikaros promoted postnatal ILC3 compartment in the gut in an Ahr-dependent manner. Ahr promoted ILC3 survival (Qiu et al., 2012); however, no enhancement of ILC3 survival was observed in *Ikzf1*$^{\Delta F4/\Delta F4}$ mice despite enhanced Ahr activity (data not shown), suggesting that Ikaros regulates ILC3s by a survival-independent mechanism and/or Ikaros deficiency counteracts the pro-survival effects of Ahr. Ahr activation also promotes the expansion of ILC3s (Kiss et al., 2011). Accordingly, ILC3 proliferation was increased in *Ikzf1*$^{\Delta F4/\Delta F4}$ mice, consistent with the enhancement of Ahr activity in *Ikzf1*$^{\Delta F4/\Delta F4}$ ILC3s. The Notch pathway is required for postnatal ILC3 differentiation from CLPs (Possot et al., 2011). In addition, Ahr activation has been shown to promote *Notch1* and *Notch2* transcription, one of the reported mechanisms by which Ahr regulates adult ILC3 compartment (Lee et al., 2012). Neither *Notch 1* or *Notch 2* transcription was affected in *Ikzf1*$^{\Delta F4/\Delta F4}$ ILC3s (data not shown). The progenitor of ILC3s, CLP, is markedly decreased in the bone marrow of *Ikzf1*$^{\Delta F4/\Delta F4}$ mice (Schjerven et al., 2013). Despite the reduction in number, CLP from the bone marrow of *Ikzf1*$^{\Delta F4/\Delta F4}$ mice appeared to more readily differentiate into ILC3s in an OP9 in vitro culturing system (data not shown). This enhanced potential of CLP to become ILC3s could also account for the increased postnatal ILC3s in the gut. Recent study demonstrated that intestinal ILC3s are tissue-resident, which are maintained and expanded locally (Gasteiger et al., 2015). Thus, Ikaros-mediated regulation of postnatal ILC3s in the gut may be different from the role of Ikaros in the bone marrow. Extrahepatic fetal ILC precursors have been identified to populate the fetal gut and become the local source of all the ILC populations (Bando et al., 2015); however, it remains to be determined whether ILC precursors can reside in the adult gut and differentiate to ILCs locally in the intestine.

Ahr is a member of the basic helix-loop-helix (bHLH)/Per-Arnt-Sim (PAS) family of proteins. Both bHLH and PAS-A domains of Ahr are thought to be involved in hetero-dimerization with ARNT; however, the PAS-A domain of Ahr has recently been demonstrated to be essential (Wu et al., 2013). Although Ikaros interacted with PAS-A domain of Ahr, no conclusive interaction could be detected between Ikaros and ARNT that also contains PAS-A domain (Li and Zhou, unpublished). Ahr repressor (Ahrr) is another member of the bHLH protein family and structurally similar to Ahr but lacks a ligand-binding domain (PAS-B domain) and an activation domain (Mimura et al., 1999). Ahrr is thought to compete with Ahr for interaction with ARNT and thus to inhibit Ahr-ARNT binding to DNA (Stockinger et al., 2014). Our data showed that Ahr-ARNT dimer was also susceptible to disruption by Ikaros, a protein that does not contain the bHLH domain or PAS-A domain. This unexpected data requires future detailed structural and biochemical characterization of the interactions among Ahr, ARNT, and Ikaros proteins without overexpression in a physiological context.

It is worthwhile to point out that our data does not rule out the possibility that the Ikaros-Ahr interaction could be inhibitory even if the interaction does not completely disrupt the Ahr-ARNT dimer, and/or Ikaros may exert its inhibitory action in ILC3 development by

Author Manuscript Author Manuscript Author Manuscript Author Manuscript

additional mechanism(s) independent of Ahr. For example, Ikaros is well known to regulate the chromatin structure of genes. In the absence of Ikaros, the chromatin structure of ILC3 target genes may be altered, thus favoring ILC3 development. Ikaros has been shown to interact with multiple proteins such as chromatin modifiers to exert its transcriptional function (Kim et al., 1999; Koipally and Georgopoulos, 2000; Naito et al., 2007; Zhang et al., 2012). Identification of Ikaros-interacting partners in ILC3s may shed light on the additional mode of regulation of ILC3s by Ikaros. Of note, Ahr interacts with RORγt that is important for Ahr recruitment to the *Il22* locus (Qiu et al., 2012). Thus, Ikaros may also participate in Ahr-RORγt complex to regulate RORγt activity in ILC3 development and/or function.

Due to Ikaros' broad expression in the hematopoietic compartment, it may regulate immune responses in a cell-type specific manner and participate the crosstalk between innate and adaptive immune systems in vivo. We observed substantial increase of NKp46^{+}RORγt^{-} cells in *Ikzf1*$^{\Delta F4/\Delta F4}$ mice, suggesting potential regulation of ILC1s by Ikaros. Given the plasticity of ILC3s (Bernink et al., 2015; Klose et al., 2014), the precise role of Ikaros in ILC1s involving its potential impact on the conversion of ILC3s to ILC1s (i.e., exILC3s) needs future investigation using *Rorc*-fate mapping mice. Our data also highlighted the complex role of Ikaros in the regulation of gut lymphocyte development and anti-bacterial immunity against *C. rodentium* that requires coordinated actions of both innate and adaptive immune cells. Our data showed that suppression of Ahr activity by Ikaros through its specific zinc finger may represent a mechanism of action of Ikaros in regulating the homeostasis of ILC3s in the gut.

Experimental procedures

Mice

All the mice in this study were maintained in Specific Pathogen Free (SPF) facilities at Northwestern University or University of Florida. Mice were littermates and were 6–8 weeks old unless otherwise indicated in the text. *Ikzf1*$^{\Delta F4/\Delta F4}$, *Ikzf1*$^{f/f}$ and *Ahr*$^{-/-}$ mice were described previously and are backcrossed to C57BL/6 background (Fernandez-Salguero et al., 1995; Heizmann et al., 2013; Schjerven et al., 2013). *Cd4*-cre mice were purchased from Taconic Farms. *Rorc*-cre mice and *Rorc*$^{gfp/gfp}$ mice were generated previously (Eberl and Littman, 2004; Sun et al., 2000). All studies with mice were approved by the Animal Care and Use Committee of Northwestern University and University of Florida.

Isolation of Intestinal Lamina Propria Lymphocytes (LPLs) and Flow Cytometry

Isolation of intestinal lamina propria cells and flow cytometry were done as previously described (Qiu et al., 2012). Flow cytometry analyses were done as described (Supplemental Information).

Immunohistology of Cryptopatches

To prepare gut tissue samples, the large and small intestines of wild-type (*Ikzf1*$^{+/+}$) or *Ikzf1*$^{\Delta F4/\Delta F4}$ mice were dissected. After removing fat tissues, intestines were cut open longitudinally and washed in PBS. Tissues were fixed in 4% paraformaldehyde in phosphate

Author Manuscript Author Manuscript Author Manuscript Author Manuscript

buffer (77 mM Na_2HPO_4, 23 mM NaH_2PO_4) with protease inhibitors (Roche) overnight, and made into Swiss rolls. The samples were then saturated in a 30% sucrose gradient overnight. The samples were embedded in OCT (Optimal Cutting Temperature, Tissue-Tek), snap frozen in a dry ice-alcohol bath, and stored at −80 C. Sections were cut3 at 5 μm and stained using human/mouse RORγt monoclonal antibody (1:200; eBioscience), anti-mouse CD3-FITC (1:800; eBioscience), and goat anti-rat IgG Cy3 (1:400; Jackson ImmunoResearch). The number of all $ROR\gamma t^{+}CD3^{-}$ cell clusters (cryptopatches) in each section were counted at 10x magnification and calculated as described (Supplemental Information).

Chromatin Immunoprecipitation (ChIP) Assay

1×10^4 sorted small intestinal ILC3s ($CD3^{-}CD45^{low}CD90^{hi}$) were treated with or without FICZ (200 nM) for 4 hours. ChIP assay was performed as described (Supplemental Information).

Plasmids, Transient Transfection, Immunoprecipitation, and Western blot

Plasmids were generated as described (Supplemental Information) and polyethylenimine (MW25000; Polysciences) were mixed at the ratio of 1:4 for 20 minutes at room temperature before adding into HEK293T cell culture medium. 24 hours later, transfected HEK293T cells were lysed in lysis buffer (1% TritonX-100, 150 mM NaCl, 20 mM HEPES [pH7.5], 1 mM EDTA) containing protease inhibitor cocktails (Roche). The lysates were immunoprecipitated with corresponding antibodies at 4°C for 3 hours and subjected to SDS-PAGE and immunobloting with Flag antibody (Sigma), HA antibody (Sigma), Ahr antibody (Novus), or ARNT antibody (Novus). To detect the dimerization between Ahr and ARNT, transfected cells were treated with or without 200 nM FICZ (Enzo) for 3 hours prior to the immunoprecipitation.

Proximity Ligation Assay (PLA)

Sorted ILC3s ($CD3^{-}CD45^{low}CD90^{hi}$) were centrifuged onto the slides using Cytospin (Thermo Scientific), fixed in 4% paraformaldehyde for 10 minutes, and then permeabilized in 1% TritonX-100 for 10 minutes. The primary antibodies against Ikaros (Hahm et al., 1998) and Ahr (goat; Santa Cruz) were used for PLA according to Duolink In Situ Probemaker Instruction (Sigma). The interaction of Ikaros and Ahr was detected using fluorescent microscope (Leica).

C. rodentium Infection and Colony-forming Units (CFUs)

C. rodentium (DBS100, ATCC51459) was cultured in LB medium overnight in shaker and the cell density was determined at OD600. Each mouse was gavaged with 10^{10} CFUs in 200 μl PBS. The survival rates and body weight were measured at indicated time points. Fecal pellets were collected, weighed and homogenized in PBS. Fecal contents were plated on MacConkey plates after serial dilution and the CFUs of *C. rodentium* were counted after incubation of plate at 37°C for 24 hours.

Author Manuscript Author Manuscript Author Manuscript Author Manuscript

DSS-induced Colitis

Mice were treated with 3% (w/v) DSS (MP Biomedicals) in drinking water for 7 days. The body weight was recorded every day to determine percentages of weight change. Colon length was measured. Middle part of the colon tissue was fixed with 10% formalin, embedded in paraffin, sectioned and stained with hematoxylin and eosin. Sections were blindly analyzed by a trained gastrointestinal pathologist. Histology scores were given with a standard described previously (Pavlick et al., 2006; Qiu et al., 2013).

Statistical Methods

Unless otherwise noted, statistical analysis was performed with the unpaired two-tailed Student's t test on individual biological samples with GraphPad Prism.

Supplementary Material

Refer to Web version on PubMed Central for supplementary material.

Acknowledgments

We thank the entire Zhou laboratory for help and suggestions, and Transgenic and Targeted Mutagenesis Laboratory (TTML) (Northwestern University) (Dr. Lynn Doglio) for services and assistance. TTML is partially supported by NIH grant CA60553 to the Robert H. Lurie Comprehensive Cancer Center at Northwestern University. We thank Drs. S. Swaminathan and C. Goolsby (Flow Cytometry Facility, Northwestern University) for cell sorting assistance, Dr. Michael Denison for providing pGudLuc6.1 luciferase plasmid and Dr. Deyu Fang for luciferase assay support. We also thank Drs. Stephen Smale and Dorina Avarm for advice and critical reading the manuscript. The work was supported by the National Institutes of Health (AI089954 and DK105562 L.Z.), and by a Cancer Research Institute Investigator Award (LZ). Liang Zhou is a Pew Scholar in Biomedical Sciences, supported by the Pew Charitable Trusts, and an Investigator in the Pathogenesis of Infectious Disease, supported by Burroughs Wellcome Fund.

References

Artis D, Spits H. The biology of innate lymphoid cells. Nature. 2015; 517:293–301. [PubMed: 25592534]

Bando JK, Liang HE, Locksley RM. Identification and distribution of developing innate lymphoid cells in the fetal mouse intestine. Nature immunology. 2015; 16:153–160. [PubMed: 25501629]

Basu R, O'Quinn DB, Silberger DJ, Schoeb TR, Fouser L, Ouyang W, Hatton RD, Weaver CT. Th22 cells are an important source of IL-22 for host protection against enteropathogenic bacteria. Immunity. 2012; 37:1061–1075. [PubMed: 23200827]

Bernink JH, Krabbendam L, Germar K, de Jong E, Gronke K, Kofoed-Nielsen M, Munneke JM, Hazenberg MD, Villaudy J, Buskens CJ, et al. Interleukin-12 and-23 Control Plasticity of CD127(+) Group 1 and Group 3 Innate Lymphoid Cells in the Intestinal Lamina Propria. Immunity. 2015; 43:146–160. [PubMed: 26187413]

Bouskra D, Brezillon C, Berard M, Werts C, Varona R, Boneca IG, Eberl G. Lymphoid tissue genesis induced by commensals through NOD1 regulates intestinal homeostasis. Nature. 2008; 456:507–U534. [PubMed: 18987631]

Collins JW, Keeney KM, Crepin VF, Rathinam VA, Fitzgerald KA, Finlay BB, Frankel G. Citrobacter rodentium: infection, inflammation and the microbiota. Nature reviews Microbiology. 2014; 12:612–623. [PubMed: 25088150]

Dere E, Lo R, Celius T, Matthews J, Zacharewski TR. Integration of genome-wide computation DRE search, AhR ChIP-chip and gene expression analyses of TCDD-elicited responses in the mouse liver. BMC genomics. 2011; 12:365. [PubMed: 21762485]

Eberl G, Littman DR. Thymic origin of intestinal alphabeta T cells revealed by fate mapping of RORgammat+ cells. Science. 2004; 305:248–251. [PubMed: 15247480]

Author Manuscript Author Manuscript Author Manuscript Author Manuscript

Fernandez-Salguero P, Pineau T, Hilbert DM, McPhail T, Lee SS, Kimura S, Nebert DW, Rudikoff S, Ward JM, Gonzalez FJ. Immune system impairment and hepatic fibrosis in mice lacking the dioxin-binding Ah receptor. Science. 1995; 268:722–726. [PubMed: 7732381]

Fukunaga BN, Probst MR, Reisz-Porszasz S, Hankinson O. Identification of functional domains of the aryl hydrocarbon receptor. The Journal of biological chemistry. 1995; 270:29270–29278. [PubMed: 7493958]

Gagliani N, Vesely MCA, Iseppon A, Brockmann L, Xu H, Palm NW, de Zoete MR, Licona-Limon P, Paiva RS, Ching T, et al. TH17 cells transdifferentiate into regulatory T cells during resolution of inflammation. Nature. 2015; 523:221–U225. [PubMed: 25924064]

Gasteiger G, Fan X, Dikiy S, Lee SY, Rudensky AY. Tissue residency of innate lymphoid cells in lymphoid and nonlymphoid organs. Science. 2015; 350:981–985. [PubMed: 26472762]

Georgopoulos K, Bigby M, Wang JH, Molnar A, Wu P, Winandy S, Sharpe A. The Ikaros Gene Is Required for the Development of All Lymphoid Lineages. Cell. 1994; 79:143–156. [PubMed: 7923373]

Guo X, Qiu J, Tu T, Yang X, Deng L, Anders RA, Zhou L, Fu YX. Induction of innate lymphoid cell-derived interleukin-22 by the transcription factor STAT3 mediates protection against intestinal infection. Immunity. 2014; 40:25–39. [PubMed: 24412612]

Hahm K, Cobb BS, McCarty AS, Brown KE, Klug CA, Lee R, Akashi K, Weissman IL, Fisher AG, Smale ST. Helios, a T cell-restricted Ikaros family member that quantitatively associates with Ikaros at centromeric heterochromatin. Genes & development. 1998; 12:782–796. [PubMed: 9512513]

Heizmann B, Kastner P, Chan S. Ikaros is absolutely required for pre-B cell differentiation by attenuating IL-7 signals. The Journal of experimental medicine. 2013; 210:2823–2832. [PubMed: 24297995]

Heller JJ, Schjerven H, Li S, Lee A, Qiu J, Chen ZM, Smale ST, Zhou L. Restriction of IL-22-producing T cell responses and differential regulation of regulatory T cell compartments by zinc finger transcription factor Ikaros. J Immunol. 2014; 193:3934–3946. [PubMed: 25194055]

Ivanov II, Diehl GE, Littman DR. Lymphoid tissue inducer cells in intestinal immunity. Current topics in microbiology and immunology. 2006; 308:59–82. [PubMed: 16922086]

Ivanov II, de Frutos RL, Manel N, Yoshinaga K, Rifkin DB, Sartor RB, Finlay BB, Littman DR. Specific microbiota direct the differentiation of IL-17-producing T-helper cells in the mucosa of the small intestine. Cell host & microbe. 2008; 4:337–349. [PubMed: 18854238]

Kanamori Y, Ishimaru K, Nanno M, Maki K, Ikuta K, Nariuchi H, Ishikawa H. Identification of novel lymphoid tissues in murine intestinal mucosa where clusters of c-kit+ IL-7R+ Thy1+ lympho-hemopoietic progenitors develop. The Journal of experimental medicine. 1996; 184:1449–1459. [PubMed: 8879216]

Kim J, Sif S, Jones B, Jackson A, Koipally J, Heller E, Winandy S, Viel A, Sawyer A, Ikeda T, et al. Ikaros DNA-binding proteins direct formation of chromatin remodeling complexes in lymphocytes. Immunity. 1999; 10:345–355. [PubMed: 10204490]

Kim MY, Kim KS, McConnell F, Lane P. Lymphoid tissue inducer cells: architects of CD4 immune responses in mice and men. Clin Exp Immunol. 2009; 157:20–26. [PubMed: 19659766]

Kiss EA, Vonarbourg C, Kopfmann S, Hobeika E, Finke D, Esser C, Diefenbach A. Natural aryl hydrocarbon receptor ligands control organogenesis of intestinal lymphoid follicles. Science. 2011; 334:1561–1565. [PubMed: 22033518]

Klose CSN, Flach M, Mohle L, Rogell L, Hoyler T, Ebert K, Fabiunke C, Pfeifer D, Sexl V, Fonseca-Pereira D, et al. Differentiation of Type 1 ILCs from a Common Progenitor to All Helper-like Innate Lymphoid Cell Lineages. Cell. 2014; 157:340–356. [PubMed: 24725403]

Koipally J, Georgopoulos K. Ikaros interactions with CtBP reveal a repression mechanism that is independent of histone deacetylase activity. Journal of Biological Chemistry. 2000; 275:19594–19602. [PubMed: 10766745]

Koipally J, Georgopoulos K. A molecular dissection of the repression circuitry of Ikaros. The Journal of biological chemistry. 2002; 277:27697–27705. [PubMed: 12015313]

Lee JS, Cella M, McDonald KG, Garlanda C, Kennedy GD, Nukaya M, Mantovani A, Kopan R, Bradfield CA, Newberry RD, Colonna M. AHR drives the development of gut ILC22 cells and

Author Manuscript Author Manuscript Author Manuscript Author Manuscript

postnatal lymphoid tissues via pathways dependent on and independent of Notch. Nature immunology. 2012; 13:144–151. [PubMed: 22101730]

Lee JS, Tato CM, Joyce-Shaikh B, Gulen MF, Cayatte C, Chen Y, Blumenschein WM, Judo M, Ayanoglu G, McClanahan TK, et al. Interleukin-23-Independent IL-17 Production Regulates Intestinal Epithelial Permeability. Immunity. 2015; 43:727–738. [PubMed: 26431948]

Lugering A, Ross M, Sieker M, Heidemann J, Williams IR, Domschke W, Kucharzik T. CCR6 identifies lymphoid tissue inducer cells within cryptopatches. Clin Exp Immunol. 2010; 160:440–449. [PubMed: 20148914]

McKenzie AN, Spits H, Eberl G. Innate lymphoid cells in inflammation and immunity. Immunity. 2014; 41:366–374. [PubMed: 25238094]

Mimura J, Ema M, Sogawa K, Fujii-Kuriyama Y. Identification of a novel mechanism of regulation of Ah (dioxin) receptor function. Genes & development. 1999; 13:20–25. [PubMed: 9887096]

Naito T, Gomez-Del Arco P, Williams CJ, Georgopoulos K. Antagonistic interactions between Ikaros and the chromatin remodeler Mi-2beta determine silencer activity and Cd4 gene expression. Immunity. 2007; 27:723–734. [PubMed: 17980631]

Pavlick KP, Ostanin DV, Furr KL, Laroux FS, Brown CM, Gray L, Kevil CG, Grisham MB. Role of T-cell-associated lymphocyte function-associated antigen-1 in the pathogenesis of experimental colitis. International immunology. 2006; 18:389–398. [PubMed: 16415103]

Pearson C, Uhlig HH, Powrie F. Lymphoid microenvironments and innate lymphoid cells in the gut. Trends in immunology. 2012; 33:289–296. [PubMed: 22578693]

Possot C, Schmutz S, Chea S, Boucontet L, Louise A, Cumano A, Golub R. Notch signaling is necessary for adult, but not fetal, development of RORgammat(+) innate lymphoid cells. Nature immunology. 2011; 12:949–958. [PubMed: 21909092]

Qiu J, Guo X, Chen ZM, He L, Sonnenberg GF, Artis D, Fu YX, Zhou L. Group 3 innate lymphoid cells inhibit T-cell-mediated intestinal inflammation through aryl hydrocarbon receptor signaling and regulation of microflora. Immunity. 2013; 39:386–399. [PubMed: 23954130]

Qiu J, Heller JJ, Guo X, Chen ZM, Fish K, Fu YX, Zhou L. The aryl hydrocarbon receptor regulates gut immunity through modulation of innate lymphoid cells. Immunity. 2012; 36:92–104. [PubMed: 22177117]

Rutz S, Wang X, Ouyang W. The IL-20 subfamily of cytokines--from host defence to tissue homeostasis. Nature reviews Immunology. 2014; 14:783–795.

Sawa S, Lochner M, Satoh-Takayama N, Dulauroy S, Berard M, Kleinschek M, Cua D, Di Santo JP, Eberl G. RORgammat+ innate lymphoid cells regulate intestinal homeostasis by integrating negative signals from the symbiotic microbiota. Nature immunology. 2011; 12:320–326. [PubMed: 21336274]

Schjerven H, McLaughlin J, Arenzana TL, Frietze S, Cheng D, Wadsworth SE, Lawson GW, Bensinger SJ, Farnham PJ, Witte ON, Smale ST. Selective regulation of lymphopoiesis and leukemogenesis by individual zinc fingers of Ikaros. Nature immunology. 2013; 14:1073–1083. [PubMed: 24013668]

Schreiber HA, Loschko J, Karssemeijer RA, Escolano A, Meredith MM, Mucida D, Guermonprez P, Nussenzweig MC. Intestinal monocytes and macrophages are required for T cell polarization in response to Citrobacter rodentium. The Journal of experimental medicine. 2013; 210:2025–2039. [PubMed: 24043764]

Serafini N, Vosshenrich CA, Di Santo JP. Transcriptional regulation of innate lymphoid cell fate. Nature reviews Immunology. 2015; 15:415–428.

Song C, Lee JS, Gilfillan S, Robinette ML, Newberry RD, Stappenbeck TS, Mack M, Cella M, Colonna M. Unique and redundant functions of NKp46+ ILC3s in models of intestinal inflammation. The Journal of experimental medicine. 2015; 212:1869–1882. [PubMed: 26458769]

Sonnenberg GF, Monticelli LA, Elloso MM, Fouser LA, Artis D. CD4(+) lymphoid tissue-inducer cells promote innate immunity in the gut. Immunity. 2011; 34:122–134. [PubMed: 21194981]

Sridharan R, Smale ST. Predominant interaction of both Ikaros and Helios with the NuRD complex in immature thymocytes. Journal of Biological Chemistry. 2007; 282:30227–30238. [PubMed: 17681952]

Author Manuscript Author Manuscript Author Manuscript Author Manuscript

Stockinger B, Di Meglio P, Gialitakis M, Duarte JH. The aryl hydrocarbon receptor: multitasking in the immune system. Annual review of immunology. 2014; 32:403–432.

Sugimoto K, Ogawa A, Mizoguchi E, Shimomura Y, Andoh A, Bhan AK, Blumberg RS, Xavier RJ, Mizoguchi A. IL-22 ameliorates intestinal inflammation in a mouse model of ulcerative colitis. The Journal of clinical investigation. 2008; 118:534–544. [PubMed: 18172556]

Sun Z, Unutmaz D, Zou YR, Sunshine MJ, Pierani A, Brenner-Morton S, Mebius RE, Littman DR. Requirement for RORgamma in thymocyte survival and lymphoid organ development. Science. 2000; 288:2369–2373. [PubMed: 10875923]

Wang JH, Nichogiannopoulou A, Wu L, Sun L, Sharpe AH, Bigby M, Georgopoulos K. Selective defects in the development of the fetal and adult lymphoid system in mice with an Ikaros null mutation. Immunity. 1996; 5:537–549. [PubMed: 8986714]

Weibrecht I, Leuchowius KJ, Clausson CM, Conze T, Jarvius M, Howell WM, Kamali-Moghaddam M, Soderberg O. Proximity ligation assays: a recent addition to the proteomics toolbox. Expert review of proteomics. 2010; 7:401–409. [PubMed: 20536310]

Wu D, Potluri N, Kim Y, Rastinejad F. Structure and dimerization properties of the aryl hydrocarbon receptor PAS-A domain. Molecular and cellular biology. 2013; 33:4346–4356. [PubMed: 24001774]

Wu L, Nichogiannopoulou A, Shortman K, Georgopoulos K. Cell-autonomous defects in dendritic cell populations of Ikaros mutant mice point to a developmental relationship with the lymphoid lineage. Immunity. 1997; 7:483–492. [PubMed: 9354469]

Yoshida T, Ng SY, Georgopoulos K. Awakening lineage potential by Ikaros-mediated transcriptional priming. Current opinion in immunology. 2010; 22:154–160. [PubMed: 20299195]

Zelante T, Iannitti RG, Cunha C, De Luca A, Giovannini G, Pieraccini G, Zecchi R, D'Angelo C, Massi-Benedetti C, Fallarino F, et al. Tryptophan catabolites from microbiota engage aryl hydrocarbon receptor and balance mucosal reactivity via interleukin-22. Immunity. 2013; 39:372–385. [PubMed: 23973224]

Zhang J, Jackson AF, Naito T, Dose M, Seavitt J, Liu F, Heller EJ, Kashiwagi M, Yoshida T, Gounari F, et al. Harnessing of the nucleosome-remodeling-deacetylase complex controls lymphocyte development and prevents leukemogenesis. Nature immunology. 2012; 13:86–94. [PubMed: 22080921]

Author Manuscript Author Manuscript Author Manuscript Author Manuscript

Highlights

- Ikaros suppresses postnatal ILC3 development in a cell-intrinsic manner.
- Suppression of ILC3 development depends on the zinc-finger 4 domain of Ikaros.
- Ikaros interacts with Ahr and inhibits Ahr transcriptional activity.
- Ikaros regulates gut immunity in a cell-type specific manner.

Author Manuscript Author Manuscript Author Manuscript Author Manuscript

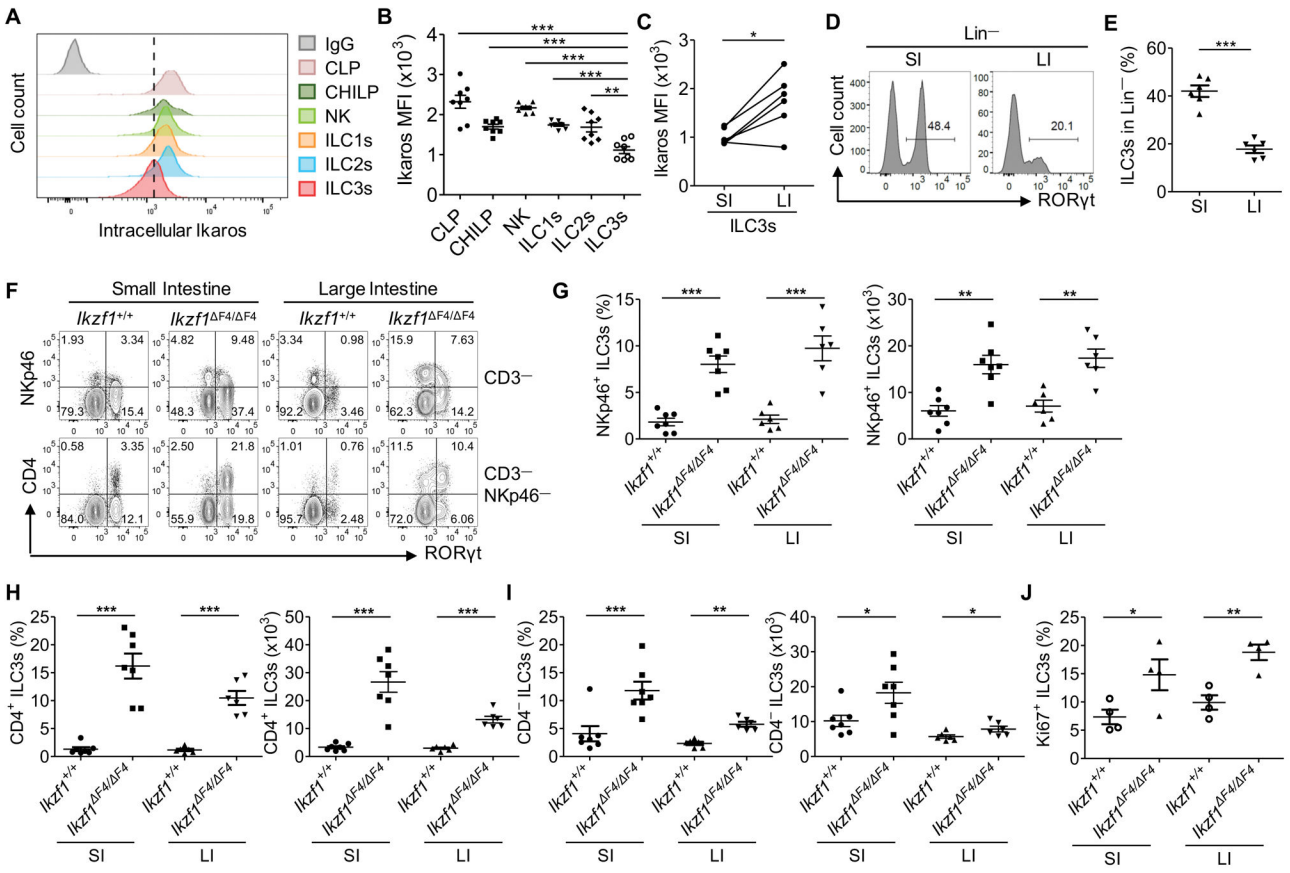

Figure 1. Reduced Ikaros expression in ILC3s and upregulation of ILC3s in *Ikzf1*$^{\Delta F4/\Delta F4}$ mice

(A) Analysis of intracellular Ikaros in CLP (Lin$^-$CD117^{low}Sca-1^{low}CD127$^+$), CHILP (Lin$^-$CD127$^+$α4β7$^+$CD25$^-$Flt3$^-$), ILC1s (Lin$^-$T-bet$^+$EOMES$^-$RORγt$^-$), NK cells (Lin$^-$T-bet$^+$EOMES$^+$RORγt$^-$), ILC2s (Lin$^-$GATA3$^+$RORγt$^-$), and ILC3s (Lin$^-$RORγt$^+$GATA3$^-$) by flow cytometry. CLP and CHILP were examined in bone marrow. ILC1s, ILC2s, and ILC3s were examined in small intestinal lamina propria leukocytes (LPLs). Data are representative of two independent experiments. Rabbit IgG isotype antibody was used to stain small intestinal ILC3s as a negative control. (B) Mean fluorescence intensity (MFI) of intracellular Ikaros in indicated populations. Data are shown as mean ± SEM (n=8 mice per group). **p<0.01, ***p<0.001. (C) MFI of intracellular Ikaros in ILC3s isolated from LPLs of the small intestine (SI) and large intestine (LI). Data were compiled from two independent experiments and are shown as mean ± SEM (n=6 mice per group). *p<0.05. (D) Flow cytometry analysis of Lin$^-$RORγt$^+$ cells in the small (SI) and large (LI) intestines. Data are representative of two independent experiments. (E) Percentages of ILC3s after gating on Lin$^-$ LPLs. Data are shown as mean ± SEM (n=6 mice per group). ***p<0.001. (F) Flow cytometry analysis of RORγt and NKp46 expression after gating on CD3$^-$ cells in LPLs of *Ikzf1*$^{+/+}$ and *Ikzf1*$^{\Delta F4/\Delta F4}$ littermate mice. CD4 and RORγt expression were analyzed after gating on CD3$^-$NKp46$^-$ cells. Data are representative of five independent experiments. (G to I) Percentages and absolute numbers of NKp46$^+$ ILC3s (NKp46$^+$RORγt$^+$ among CD3$^-$) (G), CD4$^+$ ILC3s (CD4$^+$RORγt$^+$ among CD3$^-$NKp46$^-$) (H), and CD4$^-$ ILC3s (CD4$^-$RORγt$^+$ among CD3$^-$NKp46$^-$) (I) in the small (SI) and large (LI) intestinal LPLs (n=6 to 7 mice per

Author Manuscript Author Manuscript Author Manuscript Author Manuscript

group). (J) Percentages of Ki67^{+} ILC3s (CD3^{-} RORγt^{+}) in LPLs of the small (SI) or large intestinal (LI) LPLs of *Ikzf1*$^{+/+}$ and *Ikzf1*$^{\Delta F4/\Delta F4}$ littermate mice (n=4 mice per group). Data are shown as mean ± SEM. *p<0.05, **p<0.01, ***p<0.001.
See also Figure S1.

Author Manuscript Author Manuscript Author Manuscript Author Manuscript

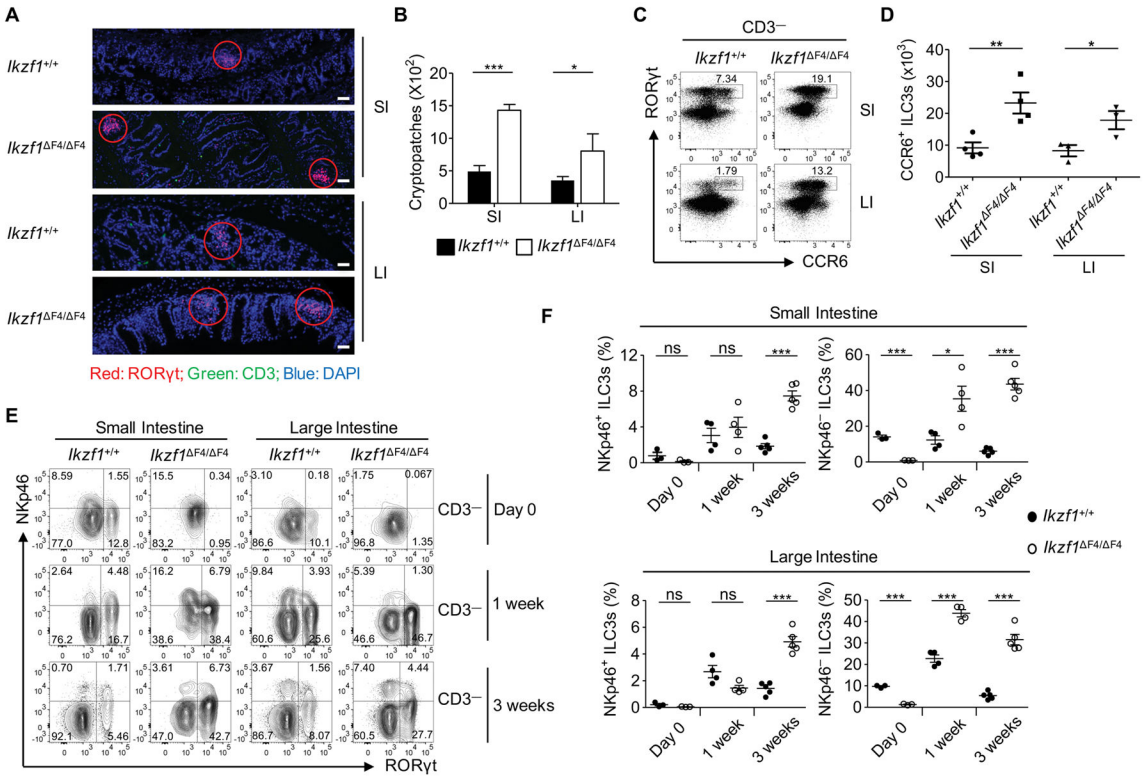

Figure 2. Increased cryptopatches and postnatal ILC3s in the gut of *Ikzf1*$^{\Delta F4/\Delta F4}$ mice

(A) Cryptopatches in representative sections of small (SI) or large intestines (LI) of *Ikzf1*$^{+/+}$ and *Ikzf1*$^{\Delta F4/\Delta F4}$ littermate mice were stained with RORγt (red), CD3 (green), and DAPI (blue) and analyzed by fluorescence microscopy. Scale bar, SI, 100 μm; LI, 50 μm. Data are representative of three independent experiments. (B) Numbers of cryptopatches in the small (SI) and large intestine (LI) of indicated mice. Data are shown as mean ± SEM (n=3 mice per group). *p<0.05, ***p<0.001. (C) Analysis of RORγt and CCR6 expression in LPLs isolated from the small (SI) and large (LI) intestines of *Ikzf1*$^{+/+}$ and *Ikzf1*$^{\Delta F4/\Delta F4}$ littermate mice after gating on CD3^{-} cells are shown. Data are representative of three independent experiments. (D) Numbers of CCR6^{+} ILC3s (CD3^{-}RORγt^{+}CCR6^{+}) in the small (SI) and large intestinal (LI) LPLs. Data are shown as mean ± SEM (n=3 to 4 mice per group). *p<0.05, **p<0.01. (E) Small and large intestinal LPLs were isolated from *Ikzf1*$^{+/+}$ and *Ikzf1*$^{\Delta F4/\Delta F4}$ littermate mice at different ages. RORγt and NKp46 expression were analyzed after gating on CD3^{-} cells. Data are representative of two independent experiments. (F) Percentage of NKp46^{+} ILC3s and NKp46^{-} ILC3s in LPLs. Data are shown as mean ± SEM (n=3 to 5 mice per group). *p<0.05, ***p<0.001.

See also Figure S2.

Author Manuscript Author Manuscript Author Manuscript Author Manuscript

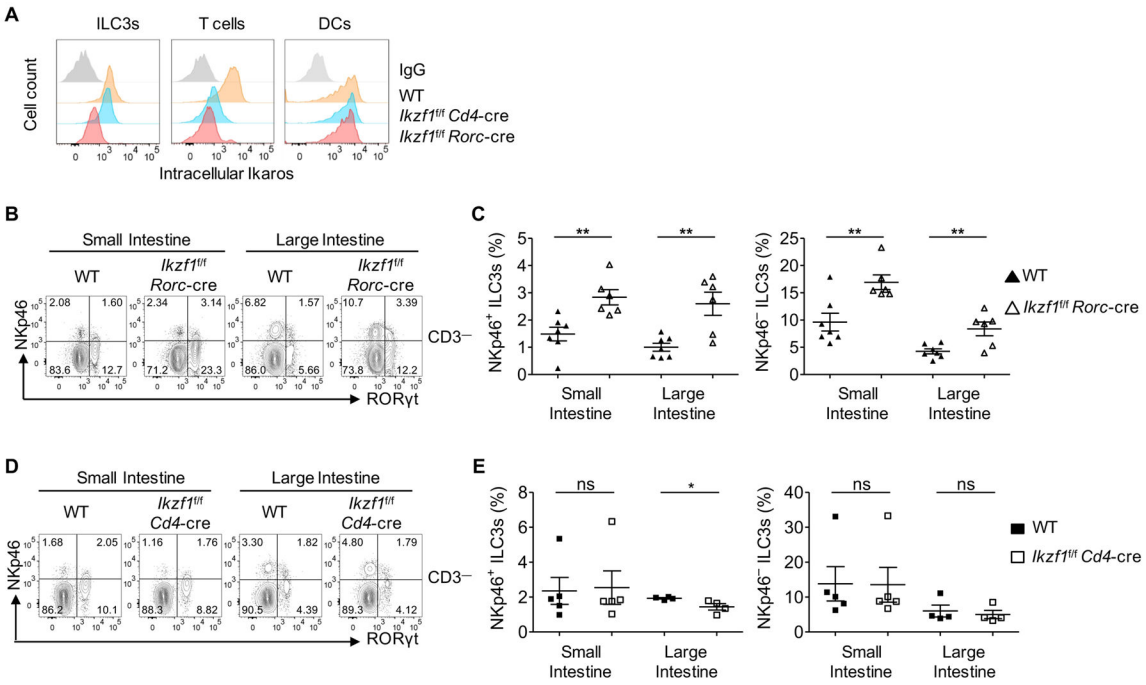

Figure 3. Ikaros inhibits intestinal ILC3s in a cell-intrinsic manner

(A) Analysis of intracellular Ikaros in ILC3s ($CD3^{-}ROR\gamma t^{+}$), T cells ($CD3^{+}$) and DCs ($CD11c^{+}MHC\text{-}II^{+}$) by flow cytometry. Rabbit IgG isotype antibody was used for each cell type as negative controls. Data are representative of two independent experiments. (B) Analysis of RORγt and NKp46 expression in LPLs from *Ikzf1*$^{f/f}$ *Rorc*-cre or wildtype (WT: *Ikzf1*$^{f/f}$ or *Ikzf1*$^{f/+}$) littermate mice after gating on $CD3^{-}$ cells. Data are representative of four independent experiments. (C) Percentages of $NKp46^{+}$ ILC3s and $NKp46^{-}$ ILC3s in the small (SI) and large intestinal (LI) LPLs (n=6 to 7 mice per group). (D) Analysis of RORγt and NKp46 expression in LPLs of *Ikzf1*$^{f/f}$ *Cd4*-cre or wildtype (WT: *Ikzf1*$^{f/f}$ or *Ikzf1*$^{f/+}$) littermate mice after gating on $CD3^{-}$ cells. Data are representative of three independent experiments. (E) Percentages of $NKp46^{+}$ ILC3s and $NKp46^{-}$ ILC3s in the small (SI) and large intestinal (LI) LPLs (n=4 to 5 mice per group). Data are shown as mean ± SEM. *p<0.05, **p<0.01.

See also Figure S2.

Author Manuscript Author Manuscript Author Manuscript Author Manuscript

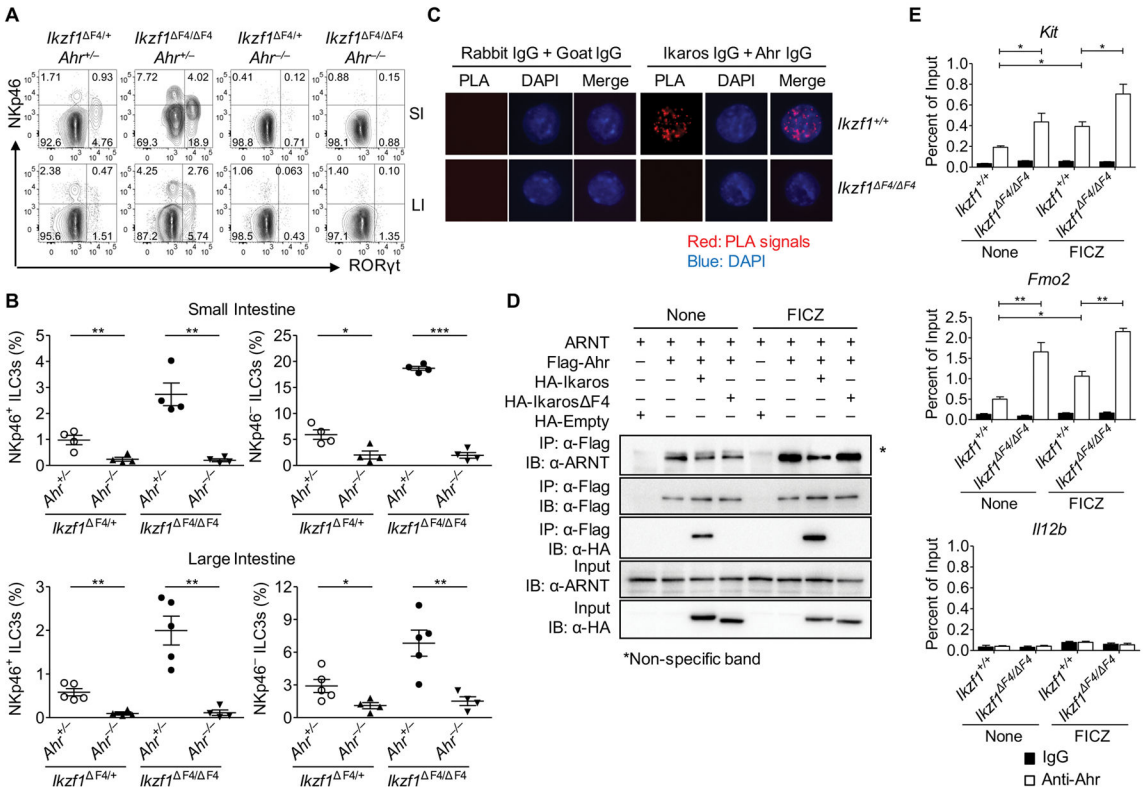

Figure 4. Ahr is required for the upregulation of ILC3s in *Ikzf1*$^{\Delta F4/\Delta F4}$ mice

(A) Analysis of RORγt and NKp46 expression in the small (SI) and large (LI) intestinal LPLs isolated from littermate mice with indicated genotypes after gating on CD3$^-$ cells. Data are representative of four independent experiments. (B) Percentages of NKp46$^+$ ILC3s and NKp46$^-$ ILC3s in the intestines of indicated mice. Data are shown as mean ± SEM (n=4 to 5 mice per group). *p<0.05, **p<0.01, ***p<0.001. (C) The interaction between Ikaros and Ahr in sorted ILC3s (CD3$^-$CD45^{low}CD90^{hi}) from *Ikzf1*$^{+/+}$ and *Ikzf1*$^{\Delta F4/\Delta F4}$ littermate mice was examined by proximity ligation assay (PLA). Data are representative of two independent experiments. (D) ARNT and Flag-tagged Ahr were expressed with HA-tagged full-length Ikaros or zinc finger 4-deleted Ikaros in HEK293T cells for 24 hours. The cells were treated with DMSO (None) or FICZ for 3 hours. Total cell lysates were immunoprecipitated (IP) with anti-Flag beads and blotted (IB) with indicated antibodies. Data are representative of two independent experiments. (E) ILC3s (CD3$^-$CD45^{low}CD90^{hi}) were sorted from the small intestine of *Ikzf1*$^{+/+}$ and *Ikzf1*$^{\Delta F4/\Delta F4}$ littermate mice. Cells were treated with DMSO (None) or FICZ for 4 hours and subjected to Ahr ChIP analysis. Enrichment of Ahr at the *Kit* promoter, *Fmo2* intron 1, and negative control *Il12b* promoter was determined by real-time PCR. Data are representative of two independent experiments. ILC3s were pooled from 2 mice per group in each experiment. Data are shown as mean ± SEM, and error bars were generated from triplicates in realtime PCR reaction. *p<0.05, **p<0.01.

See also Figures S3 and S4.

Author Manuscript Author Manuscript Author Manuscript Author Manuscript

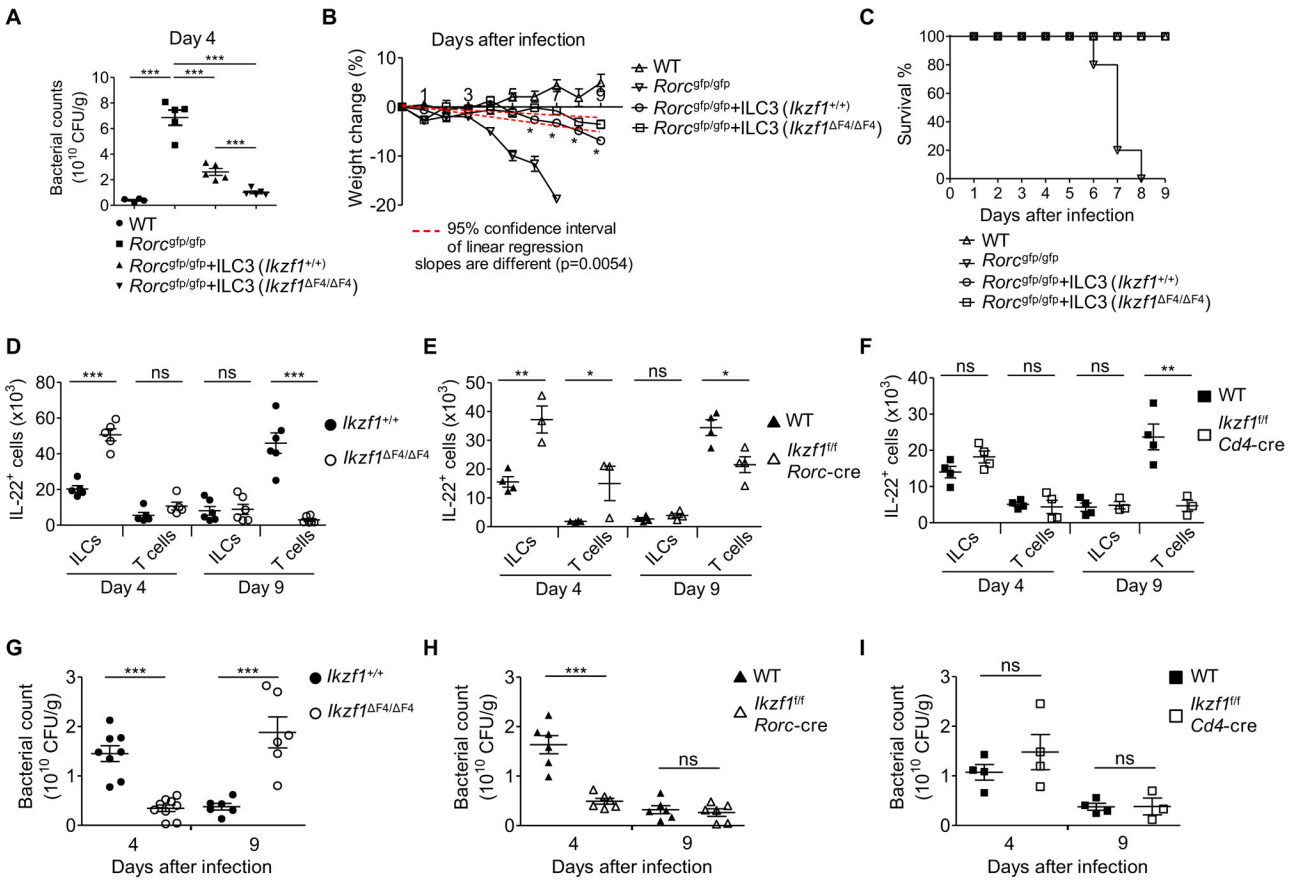

Figure 5. Ikaros regulates gut immunity against *C. rodentium* infection in a cell type-specific manner

(A to C) *Rorc*$^{gfp/gfp}$ mice were adoptively transferred with ILC3s (CD3^{-}CD45^{low}CD90^{hi}) sorted from the small intestine of *Ikzf1*$^{+/+}$ (*Rorc*$^{gfp/gfp}$ + ILC3 (*Ikzf1*$^{+/+}$)) or *Ikzf1*$^{\Delta F4/\Delta F4}$ littermate mice (*Rorc*$^{gfp/gfp}$ + ILC3 (*Ikzf1*$^{\Delta F4/\Delta F4}$)). Wildtype C57BL/6 (n=4 mice per group), and *Rorc*$^{gfp/gfp}$ with or without transfer (n=5 mice per group) were infected with *C. rodentium* 24 hours after adoptive transfer. Bacterial counts (CFUs) at day 4 (A) after infection, normalized to per gram of feces, are shown. Data are shown as mean ± SEM. ***p<0.001. Body weight changes (B) and survival rates (C) were monitored at the indicated time points. Mice were excluded from analyses after death. *p<0.05, comparing *Rorc*$^{gfp/gfp}$ + ILC3 (*Ikzf1*$^{+/+}$) group and *Rorc*$^{gfp/gfp}$ + ILC3 (*Ikzf1*$^{\Delta F4/\Delta F4}$) group (B). (D–I) *Ikzf1*$^{\Delta F4/\Delta F4}$ or *Ikzf1*$^{+/+}$ littermate mice (n=5 to 6 mice per group), *Ikzf1*$^{f/f}$ *Rorc*-cre or wildtype (WT: *Ikzf1*$^{f/f}$ or *Ikzf1*$^{f/+}$) littermate mice (n=3 to 4 mice per group), and *Ikzf1*$^{f/f}$ *Cd4*-cre or wildtype (WT: *Ikzf1*$^{f/f}$ or *Ikzf1*$^{f/+}$) littermate mice (n=3 to 4 mice per group) were infected with *C. rodentium*. IL-22^{+} ILC3s (CD3^{-}RORγt^{+}) and IL-22^{+} T cells (CD4^{+}TCRβ^{+}) were determined by flow cytometry (D–F). Bacterial counts (CFUs) were measured at day 4 or day 9 after infection and normalized to per gram of feces (G–I). Data were compiled from two independent experiments and are shown as mean ± SEM. *p<0.05, **p<0.01, ***p<0.001.

See also Figures S5 to S7.

Author Manuscript Author Manuscript Author Manuscript Author Manuscript

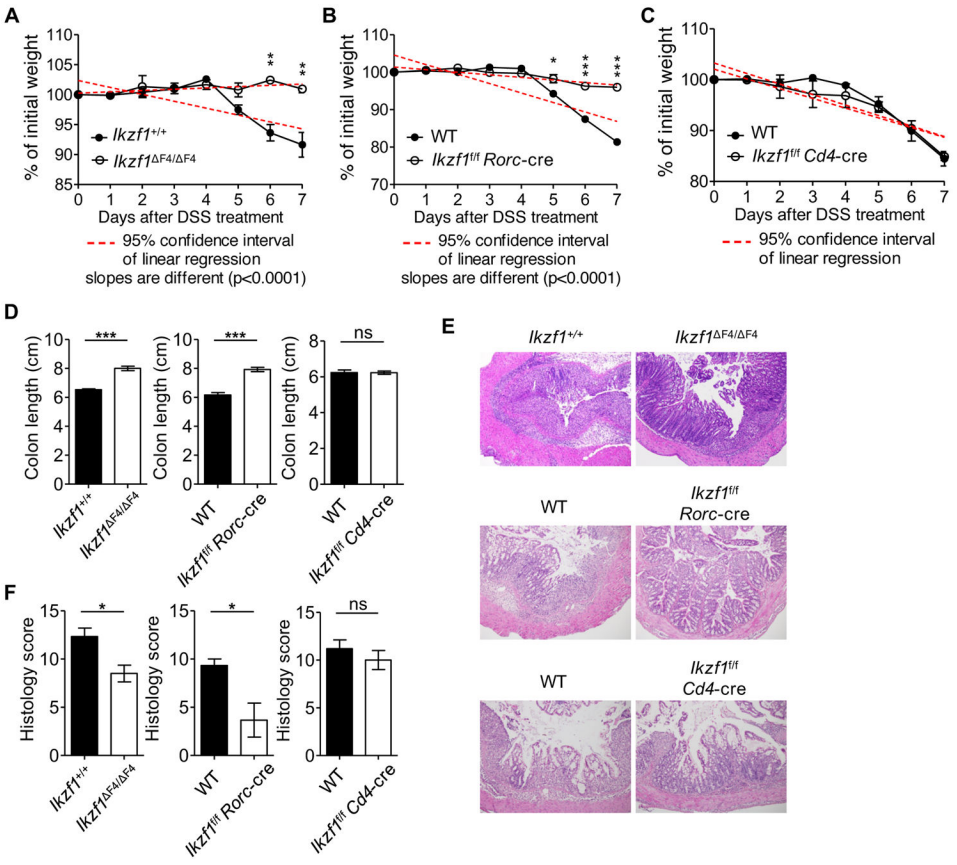

Figure 6. Ablation of Ikaros in ILC3s protects mice from DSS-induced innate colitis

Littermate mice were fed with 3% DSS water for 7 days. (A to C) Body weight changes of *Ikzf1*$^{\Delta F4/\Delta F4}$ (n=4) or *Ikzf1*$^{+/+}$ (n=4) mice, *Ikzf1*$^{f/f}$ *Rorc*-cre (n=4) or wildtype (WT: *Ikzf1*$^{f/f}$ or *Ikzf1*$^{f/+}$; n=3) mice, and *Ikzf1*$^{f/f}$ *Cd4*-cre (n=4) or wildtype (WT: *Ikzf1*$^{f/f}$ or *Ikzf1*$^{f/+}$; n=5) mice were monitored at the indicated time points. (D) Colon lengths of *Ikzf1*$^{\Delta F4/\Delta F4}$ (n=5) or *Ikzf1*$^{+/+}$ (n=4) mice, *Ikzf1*$^{f/f}$ *Rorc*-cre (n=4) or wildtype (WT: *Ikzf1*$^{f/f}$ or *Ikzf1*$^{f/+}$; n=3) mice, and *Ikzf1*$^{f/f}$ *Cd4*-cre (n=3) or wildtype (WT: *Ikzf1*$^{f/f}$ or *Ikzf1*$^{f/+}$; n=5) mice were measured. (E) Representative H&E histology sections (10X) of the colon. (F) Histology scores of *Ikzf1*$^{\Delta F4/\Delta F4}$ (n=5) or *Ikzf1*$^{+/+}$ (n=4) mice, *Ikzf1*$^{f/f}$ *Rorc*-cre (n=3) or wildtype (WT: *Ikzf1*$^{f/f}$ or *Ikzf1*$^{f/+}$; n=3) mice, and *Ikzf1*$^{f/f}$ *Cd4*-cre (n=3) or wildtype (WT: *Ikzf1*$^{f/f}$ or *Ikzf1*$^{f/+}$; n=5) mice were measured. Data were compiled from two to three independent experiments and are shown as mean ± SEM. *p<0.05, **p<0.01, ***p<0.001.

Author Manuscript Author Manuscript Author Manuscript Author Manuscript

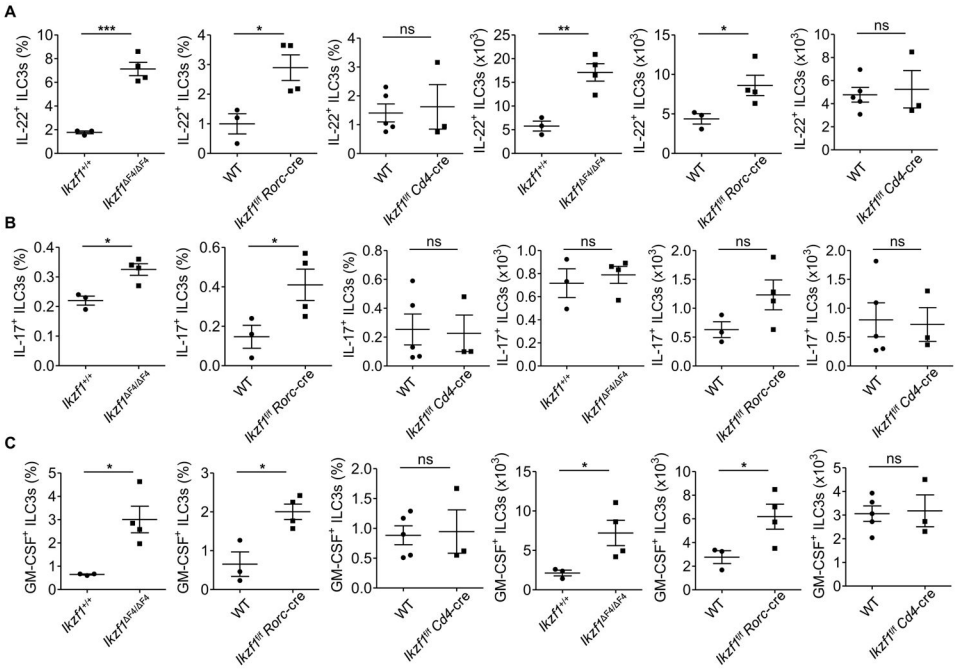

Figure 7. Enhanced cytokine production by Ikaros-deficient ILC3s during DSS-induced innate colitis

Ikzf1$^{\Delta F4/\Delta F4}$ or *Ikzf1*$^{+/+}$ littermate mice (n=3 to 4 mice per group), *Ikzf1*$^{f/f}$ *Rorc*-cre or wildtype (WT: *Ikzf1*$^{f/f}$ or *Ikzf1*$^{f/+}$) littermate mice (n=3 to 4 mice per group), and *Ikzf1*$^{f/f}$ *Cd4*-cre or wildtype (WT: *Ikzf1*$^{f/f}$ or *Ikzf1*$^{f/+}$) littermate mice (n=3 to 5 mice per group) were fed with 3% DSS water for 7 days. (A) Percentages and numbers of IL-22^{+} ILC3s in the large intestinal LPLs of indicated mice after DSS treatment are shown. (B) Percentages and numbers of IL-17^{+} ILC3s in the large intestinal LPLs of indicated mice after DSS treatment are shown. (C) Percentages and numbers of GM-CSF^{+} ILC3s in the large intestinal LPLs of indicated mice after DSS treatment are shown. Data were compiled from two independent experiments and are shown as mean ± SEM. *p<0.05, **p<0.01, ***p<0.001.